Real-time Nondestructive Evaluation of Electrode Weld Stacks using a Laser Vibrometer and Shock Tube

Han Liu[1,*], Simon Laflamme[1,2], Sarah A. Bentil[3], Robin James[4], Megan McGovern[4], Dmitriy Bruder[4]

[1] Department of Civil, Construction, and Environmental Engineering, Iowa State University, Ames, IA 50011

[2] Center for Nondestructive Evaluation, Iowa State University, Ames, IA 50021

[3] Department of Mechanical Engineering, Iowa State University, Ames, IA 50011

[4] General Motors Research and Development, 30470 Harley Earl Blvd., Warren, MI, 48092

E-mail: *liuhan@iastate.edu

March 2023

Abstract. Multi-layered electrode foil-to-tab welds in lithium-ion batteries must provide a strong structural bond as well as electrical connection. These welds can be created by ultrasonic welding, laser welding, or by a combination of the two. In this paper, the applicability of a nondestructive evaluation (NDE) method to evaluate the quality of the multi-layered electrode foils-to-tab welds is studied. The NDE method consists of exciting the electrode foils using an impulse pressure from a shock tube and measuring their resonance using a laser vibrometer. A key advantage of the technique is that it is non-contact and could be applied in real-time in a manufacturing environment. Pearson correlation coefficients are employed to evaluate the similarity between frequency spectra across different specimens of varying weld quality. Presented early results show that the NDE technique is repeatable and can be used to rank the quality of samples, and guide future research in developing a quantitative relationship between Pearson correlation coefficients and electrode weld quality.

Keywords: non-destructive evaluation (NDE), defect detection, frequency spectra, resonance, laser Doppler vibrometry, shock tube

1. Introduction

Lithium-ion battery cells are widely used in electric vehicles and comprise of an electrode stack, and the copper or aluminum [1] foils of which are joined to an external battery tab (Figure 1(a)). This is a two-step welding process where the multi-layered electrode foil stack is first joined with an ultrasonic pre-weld, then the pre-welded electrode stack is laser welded to the external tab. The most common defects in ultrasonic welds may include lack of bonding from under-welding or foil cracking/thinning from over-welding.

Laser weld defect types can include delamination, porosity, lack of nugget penetration, or foil detachment from the weld nugget which can occur due to post-weld thermal contraction (Figure 1(b)).

Weld inspection techniques can consist of destructive testing audits, such as mechanical pull testing or lap shear testing. Process monitoring techniques, such as backscattered light for laser welding [2], or parameter monitoring for ultrasonic welds [3, 4] can be used to monitor weld conditions, but do not directly detect defects. Offline methods can include imaging techniques such as optical micrographs or x-ray computerized tomography. Thermography has been shown to be an effective tool for detecting delamination in ultrasonic welds [5, 6] or porosity in laser welds [7], but it cannot currently detect foil detachment in laser welds and must be implemented in the manufacturing line immediately post-welding. Other techniques include those based on shearography [8], electrical resistance [9], and eddy current [10]. Refer to [11] for more discussion on NDE for weld defects.

The real-time inspection and evaluation of multi-layered electrode foil-to-tab welds remain challenging due to the complex weld geometry as well as rigorous set of constraints (e.g., quick, non-contact, ability to perform on very thin samples, etc.) under which the NDE technique should operate. The authors has recently proposed a real-time NDE method for 3D-printed objects by using a laser vibrometry combined with a shock tube-produced excitation to assess the quality through the evaluation of the vibration spectra, and a minimum detectable void defect of 0.039% of the object's volume was found [12]. The objective of this paper is to report preliminary results from using this technique to diagnose and quantify the condition of multi-layered electrode foils-to-tab welds, aiming at producing a technique that could quantify weld quality on-the-spot to identify and reject parts with unacceptable defects, and at eventually demonstrating the applicability of the NDE technique for deployment in an automated battery cell manufacturing setting for real-time applications.

2. Methodology

2.1. Specimens

Multi-layered electrode foil-to-tab battery weld coupons were fabricated by joining multi-layered copper foils (ultrasonically pre-welded) onto a thin aluminum tab through laser welding (Figure 1(c)), and sets of two specimens were fabricated under five different laser power levels and constant pulse width to yield five different weld conditions, and for a total of 10 specimens. Table in Figure 1 presents the normalized tensile strength measured under each laser power level and pulse width, showing that the resulting tensile strength reached the maximum value under nominal laser power and consistently decreased when the power level differed. It is important to note that "nominal" weld condition is purely defined for the purposes of this paper as a reference point and is not necessarily indicative of actual weld conditions.

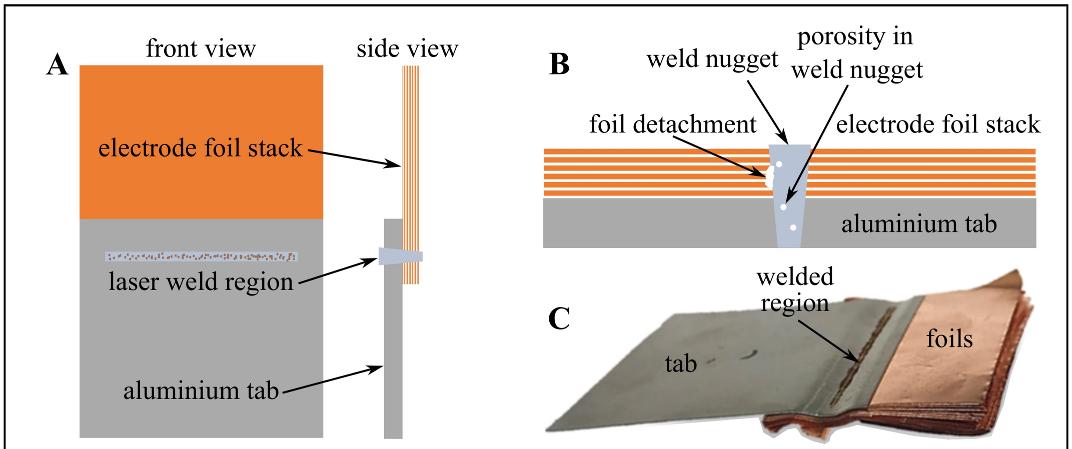

laser power	pulse width: under-weld	low-nominal	nominal	high-nominal	over-weld
under-weld	0.7477	0.8384	0.8884	0.9124	0.8919
low-nominal	0.9155	0.9771	0.9917	0.9906	0.9468
nominal	0.9468	0.9979	1.0000	0.9823	0.9928
high-nominal	0.9406	0.9823	0.9791	0.9458	0.8676
over-weld	0.9145	0.9468	0.9374	0.8947	0.8081

Figure 1. Multi-layered electrode foil-to-tab battery weld coupons and results of normalized tensile strength.

2.2. Experimental Setup

A customized compression-driven shock tube was built from a polyvinyl chloride pipe and used to generate a shock wave signal. The overall configuration and geometry of the shock tube along with a weld specimen and a laser doppler vibrometer for measuring the frequency spectra are schematized in the top of Figure 2. A shock wave is generated through the driven section by rupturing the diaphragm using an air compressor that pressurizes the air in the driver section. A laser vibrometer was aimed at the welded specimen with a stand-off distance of 306 mm to optimize the visibility of the laser to measure the vibrations of the specimen. The bandwidth and velocity range were respectively set as 100 kHz and 500 mm/s to achieve a higher data transfer rate and prevent loss of data caused by sensor saturation.

The shock tube was rigidly fixed to an optical table, and a dedicated clamp was designed to grip the specimen under a consistent gripping area. The clamp was rigidly fixed to the optical table. Two high-frequency integrated circuit piezoelectric pressure transducers were installed on the driven section to measure the incident pressure and trigger the data acquisition. A signal conditioner and oscilloscope were used to acquire data measured from the laser vibrometer, and the recording of data continued for 3000 ms with a sampling rate of 312.5 kS/s.

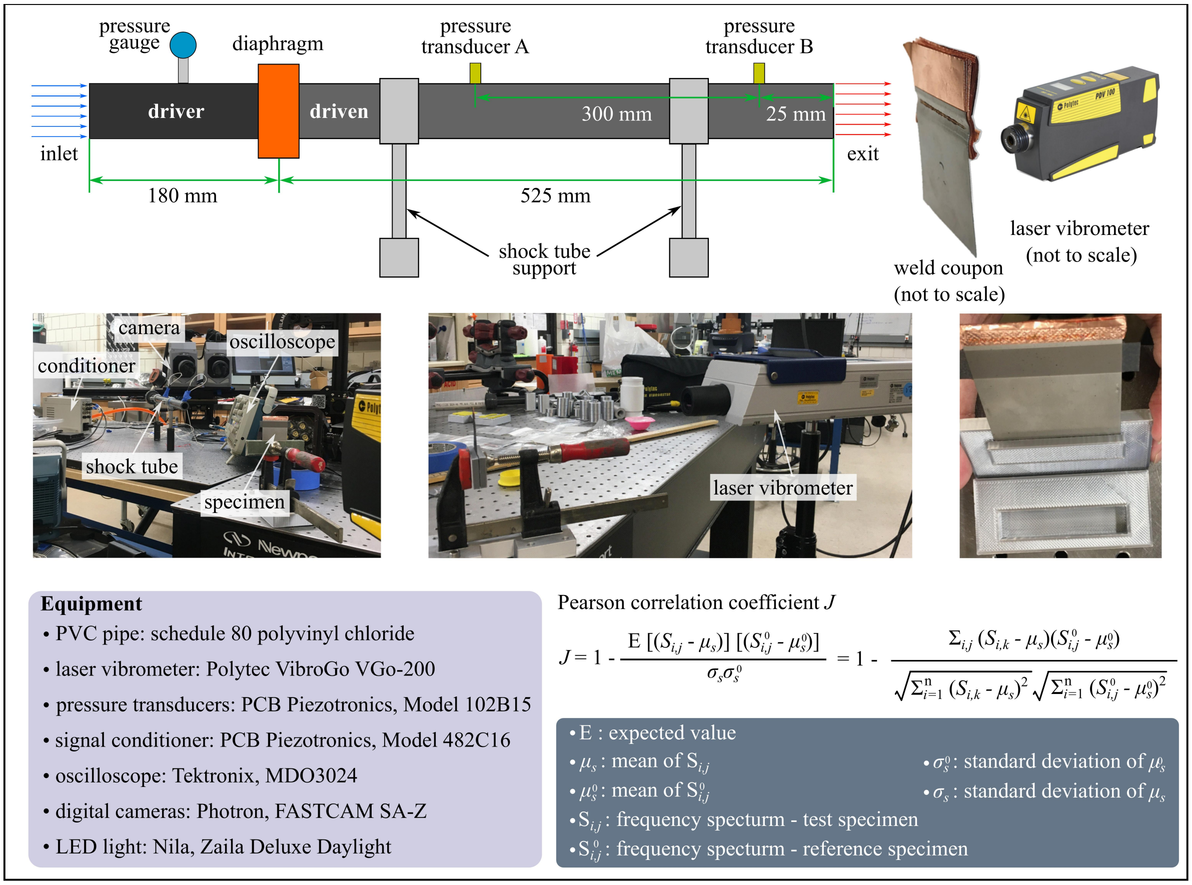

Figure 2. Experimental setup and definition of defect index J.

Digital image correlation (DIC) measurements were taken to benchmark results measured from the laser vibrometer. To do so, the welded area of the copper foil was speckled using black spray paint with a flat (i.e., matte) finish. Two synchronized high-speed digital cameras were used to image deformation and calculate vibrational velocity at a frame rate of 20,000 fps. Three tests were conducted on each specimen, for a total of six tests per laser power. Specimens were un-clamped and re-clamped between each test to investigate the repeatability of results.

3. Results and Discussion

3.1. Frequency Spectrum

Figure 3(a) presents the time series plot of the raw data obtained from a test conducted on an under-weld specimen. A damped free vibration mode can be observed after the application of the shock wave. The raw data was processed with a Tukey window to truncate the initial vibrations that may contain saturated values and minimize frequency leakage.

Figure 3(b) compares the vibration spectra of the under-weld and nominal specimens, obtained through a Fast Fourier Transform (FFT) conducted on the

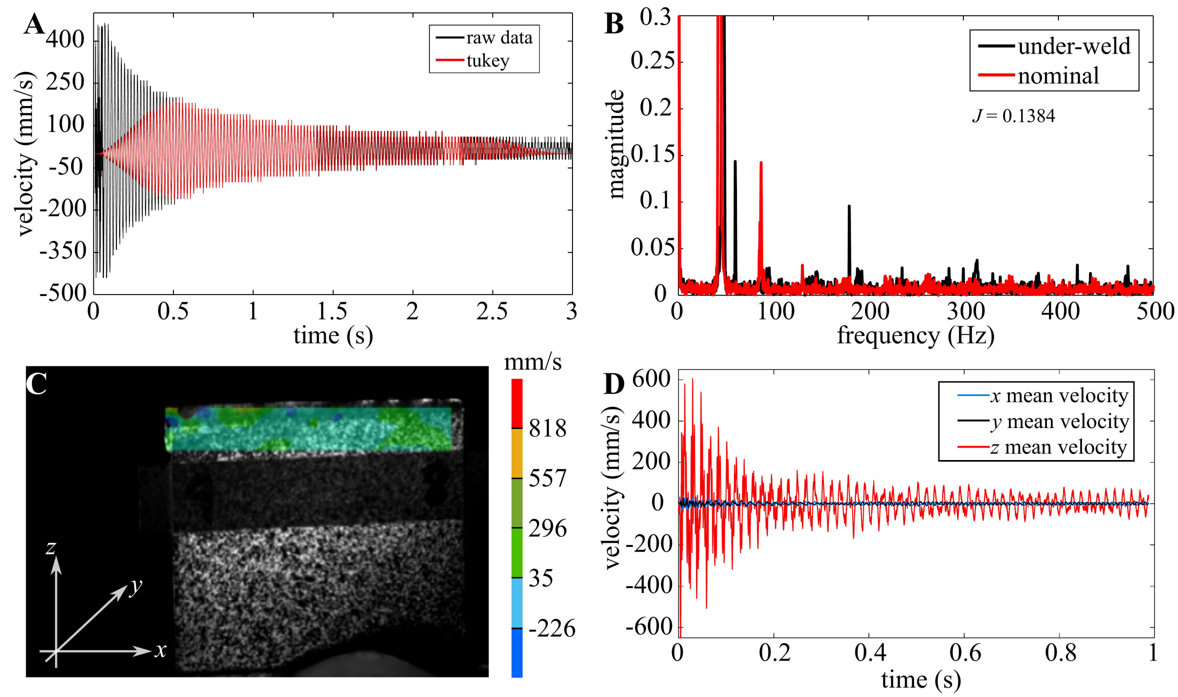

	under-weld	low-nominal	nominal	high-nominal	over-weld
under-weld	0.9413 (1.76)	0.2301 (3.25)	0.1194 (4.36)	0.1726 (2.79)	0.2941 (2.52)
low-nominal		0.9621 (3.02)	0.9133 (4.31)	0.5211 (3.29)	0.1996 (3.66)
nominal			0.9706 (2.56)	0.4191 (9.56)	0.2931 (10.20)
high-nominal				0.9408 (2.97)	0.3306 (4.08)
over-weld					0.9692 (2.76)

Figure 3. Experimental results: J along with the associated standard deviation of results written within parentheses.

windowed laser vibrometer measurements. A Pearson correlation coefficient $J = 0.1384$ was obtained, indicating a low similarity between both frequency spectra and thus discovering a 'defect'.

Figure 3(c) is a DIC plot showing the distribution of the vibration velocity in the z-direction at time $t = 0.5$ seconds after the specimen was exposed to the shock wave, with the averaged velocities along x, y, and z presented in Figure 3(d). A free vibration mode similar to the laser vibrometer measurement in terms of magnitude and decay was observed, thus validating results obtained from the laser vibrometer.

3.2. Correlation Matrix

The Pearson correlation coefficient J was adopted to quantify the similarity between two frequency spectra and thus serve as a defect index (bottom of Figure 2). The table shown in Figure 3 is the correlation matrix that displays the average J values after pruning of outliers. A total of 53 outliers (accounting for 13.1% of all measured data) were removed.

Results show that all self-correlations (along the diagonal) resulted in high J values (blue or 'no defect'), verifying the accuracy of the proposed method and the efficacy of the Person correlation coefficients. From this table, taking the nominal specimen as 'no defect', the specimen quality can be ranked as nominal (highest quality), low-nominal, high-nominal, over-weld, and under-weld (lowest quality). It follows that the correlation coefficients diminish with the laser power varying away from the nominal value, and allows for assessing and ranking specimens in terms of weld condition consistently with tensile test results reported Table in Figure 1.

The sample standard deviations of the J values computed over 36 readings (six readings per laser power level that are cross-correlated) after pruning of data is also presented in the table of Figure 3 (shown within parentheses). It can be observed that the majority of standard deviations remained below 4%, demonstrating the repeatability of results after the samples were un-clamped and re-clamped. Some of the Pearson coefficients exhibited higher standard deviations, for instance nominal versus high-nominal and over-weld, which could be attributed to uncertainties in the specimens' weld-induced defects. At this stage of the research, no CT scans were performed on the specimens to quantify defects.

4. Conclusion

This paper presented and summarized key early findings from a study on using a laser vibrometer combined with a compression-driven shock tube to detect defects and evaluate the quality of multi-layered electrode foils-to-tab welds in real-time. Results show that the frequency spectra were sensitive to the defects caused by the under-welding and over-welding. This nondestructive evaluation (NDE) technique can be potentially applied to a real-time quality control process in an automated battery cell manufacturing environment. Additional exploration must be conducted to enable in-situ applications, including the generation of validation data using CT scans, quantitatively mapping Pearson correlation coefficients to manufacturing quality, and improvement of the defect assessment algorithm by combining the analysis of additional signal features and/or machine learning capabilities.

5. Acknowledgment

The authors would like to acknowledge the financial support of the General Motors (GM) company through GM Global Academic Contract (GAC) # 3587.

References

[1] Matthew Li, Jun Lu, Zhongwei Chen, and Khalil Amine. 30 years of lithium-ion batteries. Advanced Materials, 30(33):1800561, jun 2018.

[2] Precitec. Monitoring your laser welding processes in real time. Available from: https://www.precitec.com/laser-welding/products/process-monitoring/laser-welding-monitor/, 2022 [cited 2022 June 3rd].

[3] ClosedLoop Technology Inc. Branson ultrasonic metal welding. Available from: https://cltrep.com/branson-ultrasonics/, 2020 [cited 2022 May 27th].

[4] Tech-Sonic. Closed loop technology overview (multi-step). Available from: https://tech-sonic.us/closed-loop-technology-overview/, 2021 [cited 2022 May 27th].

[5] Megan E. McGovern, , Dmitriy D. Bruder, Robin James, and Vineet Gattani. Total focusing method with laser-generated ultrasonic waves for defect detection in finite plates. In ASNT 30th Research Symposium Conference Proceedings. The American Society for Nondestructive Testing Inc., 2022.

[6] Bruder D., et al. Assessment of laser-generated ultrasonic total focusing method for battery cell foil weld inspection. (Under Review), 2022.

[7] Teresa J. Rinker, Megan E. McGovern, Tyson Brown, and Hongliang Wang. Thermographic detectability of porosity in multi-layered bare and anodized aluminum laser welds. Procedia Manufacturing, 48:165–171, 2020.

[8] Shuhai Jia, En Hong, Reuven Katz, Leonid C. Lev, Susan Smyth, and Jeffrey Abell. Nondestructive testing of ultrasonic welding joints using shearography technique. Journal of Manufacturing Science and Engineering, 134(3), may 2012.

[9] Nanzhu Zhao, Wei Li, Wayne W. Cai, and Jeffrey A. Abell. A fatigue life study of ultrasonically welded lithium-ion battery tab joints based on electrical resistance. Journal of Manufacturing Science and Engineering, 136(5), aug 2014.

[10] Erik Rohkohl, Mathias Kraken, Malte Schönemann, Alexander Breuer, and Christoph Herrmann. How to characterize a NDT method for weld inspection in battery cell manufacturing using deep learning. The International Journal of Advanced Manufacturing Technology, 119(7-8):4829–4843, jan 2022.

[11] Megan E. McGovern, Dmitriy D. Bruder, Erik D. Huemiller, Teresa J. Rinker, Jennifer T. Bracey, Ryan C. Sekol, and Jeffrey A. Abell. A review of research needs in nondestructive evaluation for quality verification in electric vehicle lithium-ion battery cell manufacturing. Journal of Power Sources, 561:232742, mar 2023.

[12] Han Liu, Simon Laflamme, Carter Morgan, Matthew Nelson, and Sarah A. Bentil. Real-time nondestructive evaluation of additive manufacturing using a laser vibrometer and shock tube. Journal of Nondestructive Evaluation, Diagnostics and Prognostics of Engineering Systems, 6(1), oct 2022.